2014 IEEE 80th Vehicular Technology Conference (VTC2014-Fall) (2014)
pp.1-6
DOI:10.1109/VTCFall.2014.6966148

Radio-over-Fiber Aided Base Station Coordination for OFDM

Ana Garcia Armada[+], Varghese Antony Thomas[≈], Mohammed El-Hajjar[≈] and Lajos Hanzo[≈]

[+] University Carlos III of Madrid, Department of Signal Theory and Communications
e-mail: agarcia@tsc.uc3m.es

[≈] School of ECS, University of Southampton, SO17 1BJ, United Kingdom.
e-mail: }vat1g10,meh,lh |@ecs.soton.ac.uk

***Abstract*—Radio over Fiber (RoF) distribution aided co-operation of Remote Access Points (RAPs) is proposed for jointly transmitting data to the users in the downlink (DL) of a Multiple Input Multiple Output Orthogonal Frequency Division Multiplexing (MIMO-OFDM) system. Joint transmission is performed with the aid of Block Diagonalization (BD), where the transmitted signal is pre-distorted in order to overcome the non-linearity imposed by the optical modulator. We demonstrate that with adequate design, the users can obtain high data rates with very small degradation introduced by the RoF transmission. Quantitatively, when $M = 7$ RAPs, each equipped with $t = 2$ transmit antennas (TAs) each, cooperate to serve $N = 7$ simultaneous users, also equipped with $r = 2$ receive antennas (RAs), the SNR degradation is kept below 0.1 dB compared to a system assuming a perfect RoF channel. On the other hand, the SNR performance degradation is around 1.2 dB, when the number of antennas at the transmitters and the receivers is increased to $t = r = 8$.** [1]

***Index Terms*—Radio over Fiber, Coordinated MultiPoint, Network MIMO, multiple-antennas, Block Diagonalization.**

I. Introduction

Multiple Input-Multiple Output (MIMO) techniques have emerged as a means of achieving high-capacity communications with the aid of Spatial Division Multiplexing (SDM) [1]. However, the introduction of MIMO-SDM in practical cellular networks has entirely not achieved the benefits estimated on the basis of idealized simplifying conditions, amongst others, since it requires high Signal-to-Noise-plus-Interference Ratios (SINR). Some recent studies have focused on managing the interference in radical cellular systems relying on a frequency reuse factor of unity, by introducing coordination among the Base Stations (BSs) in the downlink (DL). These BS coordination techniques are typically referred to as 'network-MIMO' techniques [4], [5] or Coordinated MultiPoint (CoMP) schemes [6]. If the DL channel is known at the transmitters, then cooperative encoding among the BSs using Dirty Paper Coding (DPC) is capable of suppressing the Other Cell Interference (OCI) [3]. However for complexity reasons, typically linear precoders are preferred. In this work, we will rely on the Block Diagonalization (BD) technique of [7], [8], [12], which has been shown to asymptotically approach the performance achieved using DPC.

Block diagonalization requires both the data and the Channel State Information (CSI) to be shared amongst the cooperating cells. The performance achieved using BD improves, as the number of cooperating BSs increases. On the other hand, in order to reduce the signalling and back-haul requirements, coordination may be accomplished in clusters of reduced size. It was shown in [9], [10] that a cluster size of 7 cells may be a beneficial compromise between the complexity imposed and the performance attained.

[1]This work was supported by projects CSD2008-00010, TEC2011-29006-C03-03 and by a mobility grant of Spanish Ministry of Education. The financial support of the UK Government's Engineering & Physical Sciences Research Council (EPSRC) as well as that of the Research Councils UK (RCUK) and of the European Research Council's Senior Research Fellow Grant is also gratefully acknowledged.

Both the number as well as the bandwidth demand of the wireless devices has increased rapidly over the last few years. The use of a large number of small cells is the most viable solution to the challenge of serving a larger number of users. A full-fledged BS is costly, especially in the event of migration to high RF carriers to exploit the hitherto un-utilised spectrum. Having a large number of such BSs serving these small cells would result in an excessive installation cost for the service provider. Radio over Fiber (RoF) constitutes a potential solution to this economic challenge, which is hence investigated in this paper. This technique employs Radio Access Points (RAPs) that perform only modest signal processing to serve the cells, while most of the high-complexity signal processing is concentrated in a centralised BS [20]. This way, both the RAP intelligence and its costs are reduced. As a benefit, the resultant pico- and femto-cell RAPs may be endowed with the possibility of cooperating, while hardware sharing at the BS reduces the network's cost. This is important, since the number of small cells is increasing, with about 3 million small cell-installations being forecast in 2016 [11]. Thus, in this contribution, the computation of the transmit precoders (TPCs) and the joint DL encoding process will be performed in a centralized way at the BS. Moreover, hardware sharing at the BS makes any system upgrades easy, while centralised signal processing is capable of supporting efficient resource allocation through the use of dynamic algorithms. Other advantages of such an architecture include the ability to exploit the low attenuation and large bandwidth of the optical fiber, seamless wireless coverage as well as high power efficiency [20]. Additionally, the existing fiber-based optical networks can also be exploited, because these networks carry baseband digital data, while the RoF scheme transmits RF signals.

In this paper we focus on the DL, where we propose the employment of RoF transmission for RAP cooperation in cellular networks, while keeping the cost low. We use an idealized BD aided system with a perfect backhaul [10], [12] as our benchmarker for a 5 MHz bandwidth Long Term Evolution (LTE) standard DL, where $M = 7$ RAPs, each equipped with $t = 2$ transmit antennas (TAs), cooperate to serve $N = 7$ simultaneous users, each having $r = 2$ receive antennas (RAs). We will show that the RoF-induced Signal to Noise Ratio (SNR) degradation is kept below 0.1 dB, while it is around 1.2 dB, when the number of antennas at both the transmitters and receivers is increased to $t = r = 8$. Moreover, we show that the performance degradation, does not change when increasing the fiber length up to 30 km. In [13] the performance of RoF links using low cost optoelectronic components is assessed for an OFDM system without cooperation of the RAPs. The cost and performance of RoF links for this application is compared with alternative link types that use digitized radio transmission and it is shown that RoF is the optimum choice from a cost perspective. On the other hand [14] shows a different design where MIMO wireless signals are sent via different fibre modes to the RAPs over a single multimode fibre using mode division multiplexing.

The rest of the paper is organized as follows. The signal model,

the BD precoding, the RoF transmission and the receiver processing are described in Section II. Then, the design of the RoF link is detailed, along with the selection of its main parameters and with the discussion of their impact on the overall performance. Our numerical results characterizing the complete system, that relies on a MIMO-OFDM signal following the LTE standard, are discussed in Section IV, followed by our concluding remarks.

Notation: The following notation will be used in this paper. Boldface symbols will be used for matrices and vectors, while italic letters will be used for scalars. Superscripts $^{\mathrm{T}}$ and $^{\mathrm{H}}$ denote the transpose and the Hermitian transpose of a matrix, respectively.

II. System Model

We consider a network-MIMO-aided DL scenario, where M RAPs are organized in a cluster of M cells having a radius of R_{cell} and serve N Mobile Stations (MSs), or users. Each RAP is equipped with t TAs and each MS has r RAs. Figure 1 shows an example of such a cluster layout.

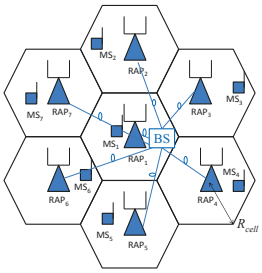

Fig. 1. **Cluster made of $M = 7$ cells with $t = 2$ TAs per RAP and $N = 7$ MSs with $r = 1$ RAs each.**

A BS is responsible for computing the TPC weights using the CSI knowledge, that has been gathered at each RAP and fed back to the BS. The BS is also responsible for generating the RF signals that will be transmitted from each of the t TAs in the M RAPs. These RF signals are transmitted from the BS to each of the RAPs through a RoF link, which is illustrated in Figure 2.

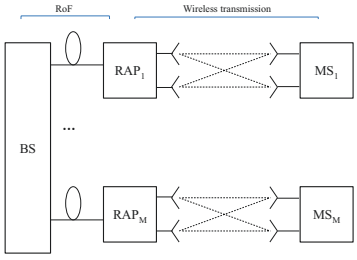

Fig. 2. **Illustration of the complete system - RoF and wireless transmission.**

A. Signal Model

Using the LTE standard [15] as our wireless system model, the transmitted DL signal is Orthogonal Frequency Division Multiplexing (OFDM) modulated, where we use N_{OFDM} subcarriers in our proposed system with a subcarrier spacing of 15 kHz. Let us denote the subcarrier index as p, with $p = 1,\ldots,N_{OFDM}$, and group the signals of subcarrier p, that are received by each of the Nr RAs of the cluster[2] in a $(Nr*1)$-element vector $\boldsymbol{y}^p$. Then, the received signal vector $\boldsymbol{y}^p$ may be expressed as:

$$\boldsymbol{y}^p = \boldsymbol{H}^p \boldsymbol{x}^p + \boldsymbol{n}^p, \tag{1}$$

where $\boldsymbol{x}^p$ is the $(Mt*1)$-element transmit signal vector, generated by grouping the signals that are transmitted on the p-th subcarrier from the set of t TAs in each of the M RAPs in the cluster. Furthermore, $\boldsymbol{n}^p$ is the $(Nr*1)$-element independent and identically distributed (i.i.d) complex Gaussian noise vector that corrupts the signal in the p-th subcarrier, whose elements have zero-mean and a variance of σ^2. We define $\boldsymbol{H}_k^p$, with $k = 1\ldots N$, as the $(r*Mt)$-element channel matrix that characterizes the propagation from all the t TAs of the M RAPs to the r RAs of MS k on the p-th subcarrier. Hence, the channel experienced by each subcarrier p may be modelled by the $(Nr*Mt)$-element matrix $\boldsymbol{H}^p$, where each matrix coefficient represents the fading in the wireless channel from each TA in each RAP to each RA in each MS. Mathematically, $\boldsymbol{H}^p$ can be represented as:

$$\boldsymbol{H}^p = \left]\boldsymbol{H}_1^{p\mathrm{T}} \boldsymbol{H}_2^{p\mathrm{T}} \ldots \boldsymbol{H}_N^{p\mathrm{T}}\right\rangle^{\mathrm{T}}. \tag{2}$$

Additionally, the Signal to Noise Ratio (SNR) can be expressed as:

$$\rho = \frac{E[\boldsymbol{x}^{p\mathrm{H}} \boldsymbol{H}^{p\mathrm{H}} \boldsymbol{H}^p \boldsymbol{x}^p]}{\sigma^2}. \tag{3}$$

B. Block Diagonalization and Power Allocation

According to (1), the signal received at each MS is composed of the useful DL signal received from the RAP to which the MS is attached plus the interference coming from other RAPs in the cluster. Hence, in order to eliminate the interference, the transmitted signal is precoded as follows:

$$\boldsymbol{x}^p = \sum_{i=1}^{r} b_{1i}^p \boldsymbol{w}_{1i}^p + \sum_{i=1}^{r} b_{2i}^p \boldsymbol{w}_{2i}^p + \times\times\times + \sum_{i=1}^{r} b_{Ni}^p \boldsymbol{w}_{Ni}^p = \boldsymbol{W}^p \boldsymbol{b}^p, \tag{4}$$

where b_{ki}^p represents the i-th symbol for user k that is transmitted with power P_{ki}^p on the p-th subcarrier and $\boldsymbol{w}_{ki}^p = \left]w_{ki}^{p,1},\ldots,w_{ki}^{p,(m\ \ 1)t+j},\ldots,w_{ki}^{p,Mt}\right\rangle^{\mathrm{T}}$ are the precoding vectors, where $w_{ki}^{p,(m\ \ 1)t+j}$ is the weight of j-th TA $(j = 1\ldots t)$ of the m-th RAP for the i-th symbol of the k-th user that is transmitted on the p-th subcarrier. The TPC matrix $\boldsymbol{W}^p = \left]\boldsymbol{w}_{11}^p,\ldots,\boldsymbol{w}_{1r}^p,\ldots,\boldsymbol{w}_{k1}^p,\ldots,\boldsymbol{w}_{kr}^p,\ldots,\boldsymbol{w}_{N1}^p,\ldots,\boldsymbol{w}_{Nr}^p\right|$ will be obtained under the BD criterion, as detailed in [12] in order to guarantee that we have:

$$\boldsymbol{H}_k^p \left]\boldsymbol{w}_{q1}^p, \boldsymbol{w}_{q2}^p \ldots \boldsymbol{w}_{qr}^p\right\rangle = \begin{pmatrix} \boldsymbol{0} & : & k \neq q \\ \boldsymbol{U}_k^p \boldsymbol{S}_k^p & : & k = q, \end{pmatrix} \tag{5}$$

where $\boldsymbol{U}_k^p$ is a unitary matrix and $\boldsymbol{S}_k^p = \mathrm{diag}\left\}\ \lambda_{k1}^{p\left[1/2\right.}, \lambda_{k2}^{p\left[1/2\right.},\ldots, \lambda_{kr}^{p\left[1/2\right|}\right.$ is a diagonal matrix that contains the square roots of the non-zero eigenvalues of the matrix $\boldsymbol{Q}_k^p \boldsymbol{Q}_k^{p\mathrm{H}}$, where $\boldsymbol{Q}_k^p$ is the part of the channel matrix $\boldsymbol{H}_k^p$ that is orthogonal to the subspace spanned by the other users' channels $\boldsymbol{H}_q^p$ with $q \neq k$ [12].

Then, the signal received on the p-th subcarrier can be expressed as:

$$\boldsymbol{y}^p = \begin{bmatrix} \boldsymbol{U}_1^p \boldsymbol{S}_1^p & \boldsymbol{0} & \ldots & \boldsymbol{0} \\ \boldsymbol{0} & \boldsymbol{U}_2^p \boldsymbol{S}_2^p & \ldots & \boldsymbol{0} \\ \vdots & \vdots & \ddots & \vdots \\ \boldsymbol{0} & \boldsymbol{0} & \ldots & \boldsymbol{U}_N^p \boldsymbol{S}_N^p \end{bmatrix} \tilde{\boldsymbol{b}}^p + \boldsymbol{n}^p, \tag{6}$$

[2]A cluster is formed of M RAPs with t TAs each serving N MSs with r RAs each. Hence, there are a total of Mt TAs and Nr RAs.

where each MS may independently rotate the received signal and hence decouple the different streams. Thus, the signal obtained by the k-th MS on p-th subcarrier can be expressed as:

$$\boldsymbol{y}_k^p = \boldsymbol{U}_k^{p\mathrm{H}} \boldsymbol{S}_k^p \boldsymbol{b}_k^p + \boldsymbol{n}_k^p = \begin{bmatrix} \lambda_{k1}^p & & \\ & \ddots & \\ & & \lambda_{kr}^p \end{bmatrix}^{1/2} \begin{bmatrix} b_{k1}^p \\ \vdots \\ b_{kr}^p \end{bmatrix} + \boldsymbol{n}_k^p, \tag{7}$$

where the noise $\boldsymbol{n}_k^p$ remains 'white' with the same covariance of $\boldsymbol{n}^p$, because we use a unitary transformation [12]. Then, the overall system will be composed of a set of parallel non-interfering channels, where the achievable rates per user with N_{OFDM} allocated subcarriers can be expressed as follows:

$$R_k = \frac{1}{N_{OFDM}} \sum_{p=1}^{N_{OFDM}} \sum_{i=1}^{r} \log_2 \left(1 + \frac{\lambda_{ki}^p P_{ki}^p}{\sigma^2 \Gamma}\right), \tag{8}$$

where Γ is the so-called SNR discrepancy [17], quantifying how far the transmission rates are from Shannon's capacity at a given error probability, for a specific modulation and channel coding scheme. In order to guarantee that k_{bits} bits are transmitted on each of the data streams and subcarriers with a given error probability, that implies a given Γ, the following power allocation is used for all data streams $k = 1 \ldots N$, $i = 1 \ldots r$ and subcarriers $p = 1 \ldots N_{OFDM}$:

$$P_{ki}^p = \frac{(2^{k_{bits}} - 1)\sigma^2 \Gamma}{\lambda_{ki}^p}. \tag{9}$$

Once the TPC matrix $\boldsymbol{W}$ and the power P_{ki}^p allocated to each data stream have been determined in the BS, the Mt precoded OFDM vectors $\boldsymbol{X}_{mj}$, with $m = 1 \ldots M$ and $j = 1 \ldots t$, and the components $X_{mj}[n]$, with $n = 1 \ldots N_{OFDM}$, are obtained from the components x_{mj}^p of the precoded vector $\boldsymbol{x}^p$ using the following expression:

$$X_{mj}[n] = \frac{1}{N_{OFDM}} \sum_{n=1}^{N_{OFDM}} x_{mj}^p e^{-\frac{j2\pi}{N_{OFDM}} np}. \tag{10}$$

Finally, a cyclic prefix of length N_{CP} is concatenated to each of the signals, which are subsequently upconverted to the transmission frequency f_0, serially concatenated and Digital-to-Analogue converted for transmission to the RAPs through the RoF link. We denote the RF signal to be transmitted using the RoF technique as $V_{RF}(t)$.

C. Radio over Fiber Tranmission

Fig. 3 shows the block diagram of the RoF DL transmitting data from the BS to the RAP, where the electronic RF signal $V_{RF}(t)$ generated at the BS is pre-distorted to mitigate the non-linearity imposed by the optical modulator. The pre-distorted signal $V_{dist}(t)$ is then used for modulating the intensity of an optical carrier generated by the Laser Diode (LD), as shown in Figure 3. Subsequently, the optical signal propagates through the fiber to the RAP for photo-detection. Afterwards, the photo-detected signal is filtered, amplified and transmitted to the MS over the wireless channel. The components of the RoF link shown in Fig. 3 are described in detail in the following sections.

1) Optical Modulation: A $f_c = \frac{\omega_c}{2\pi}$ Hz laser having an optical transmit power of P_{laser} has an ideal optical field of $E_{laser}(t)$, which is mathematically expressed as [21]:

$$E_{laser}(t) = \sqrt{2P_{laser}} e^{j\omega_c t}. \tag{11}$$

The output of the laser diode, represented by LD in Fig. 3, is fed to a dual-drive Mach-Zehnder Modulator (MZM), which is the optical modulator used in the proposed architecture. As shown in Fig. 3, the pre-distorted signal $V_{dist}(t)$ is added to the bias voltage V_{bias} for generating the total drive voltage $V(t) = V_{bias} + V_{dist}(t)$. Both arms of the dual-drive MZM are made of a material like Lithium Niobate ($LiNbO_3$), where a propagating optical signal experiences a refractive index that can be varied by varying the voltage applied to the material. The voltage $V(t)$ is applied differentially to the two arms of the MZM shown in Fig. 3 using the voltages of $V_1(t)$ and $V_2(t)$, i.e. $V(t) = V_1(t) \quad V_2(t)$. For an MZM having an insertion loss of t_{attn} dB, the exiting optical signal's field $E_{MZM}(t)$ and intensity $P_{MZM}(t)$ can be expressed as follows [21]:

$$\begin{aligned} P_{MZM}(t) &= \left|E_{MZM}(t)\right|^2 \\ &= \left|\frac{E_{laser}(t) \quad \sqrt{t_{attn}}}{2}\right| e^{j\pi \frac{V_1(t)}{V_\pi}} + \gamma e^{j\pi \frac{V_2(t)}{V_\pi}} \Bigg\}^2, \\ &= \frac{P_{laser} t_{atten}}{2} [1 + \gamma^2 + 2\gamma \cos(\frac{\pi(V_1(t) \quad V_2(t))}{V_\pi})] \\ &= \frac{P_{laser} t_{atten}}{2} [1 + \gamma^2 + 2\gamma \cos(\frac{\pi(V_{bias} + V_{dist}(t))}{V_\pi})], \end{aligned} \tag{12}$$

where V_π is typically termed as the switching voltage of the MZM, because it is the voltage which, upon being applied to the arm of a MZM, results in a phase change of π radians in the signal propagating in that arm. Furthermore, $\gamma = (\sqrt{\varepsilon} \quad 1)/(\sqrt{\varepsilon} + 1) \; / \; 1$, where ε is the extinction ratio of the MZM, i.e. the ratio of the maximum to the minimum optical power output of the MZM. Ideally we would like to have, $\varepsilon = \infty$, which would result in $\gamma = 1$. Fig. 4 shows how the output optical power varies with the drive voltage $V(t)$. The proposed architecture employs the Optical Double Sideband (ODSB) intensity modulation scheme, which requires a bias voltage of $V_{bias} = V_\pi/2$. Thus, Equation (12) can be simplified to:

$$P_{MZM}(t) = \frac{P_{laser} t_{atten}}{2} [1 + \gamma^2 \quad 2\gamma \sin(\frac{\pi V_{dist}(t)}{V_\pi})]. \tag{13}$$

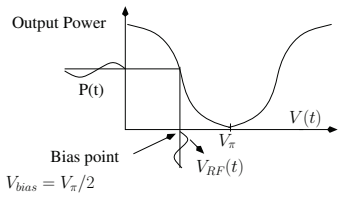

Fig. 4. MZM transmittance curve

If MDV is the maximum value of the pre-distorted drive signal, then $\frac{MDV}{V_\pi}$ is referred to as the depth of optical modulation. As seen from Fig. 4 and Equation (13), the transfer function of the MZM is nonlinear, which would result in the generation of both intermodulation products as well as in upper harmonics and would also limit the optical modulation depths that can be employed. However, the employment of the pre-distortion filter overcomes this challenge, where the proposed architecture employs an inverse-sine filter similar to the one used in [18].

2) Optical Fiber Channel: The modulated optical signal propagates from the BS to the RAP through a single-mode optical fiber, which is characterized by the following Non-Linear Schrödinger (NLS) equation [19]:

$$\begin{aligned} \frac{\partial A(z,T)}{\partial z} = \quad & \frac{\alpha}{2} A(z,T) \quad i\frac{\beta_2}{2} \frac{\partial^2 A(z,T)}{\partial T^2} \\ & + i\gamma \left|A(z,T)\right|^2 A(z,T). \end{aligned} \tag{14}$$

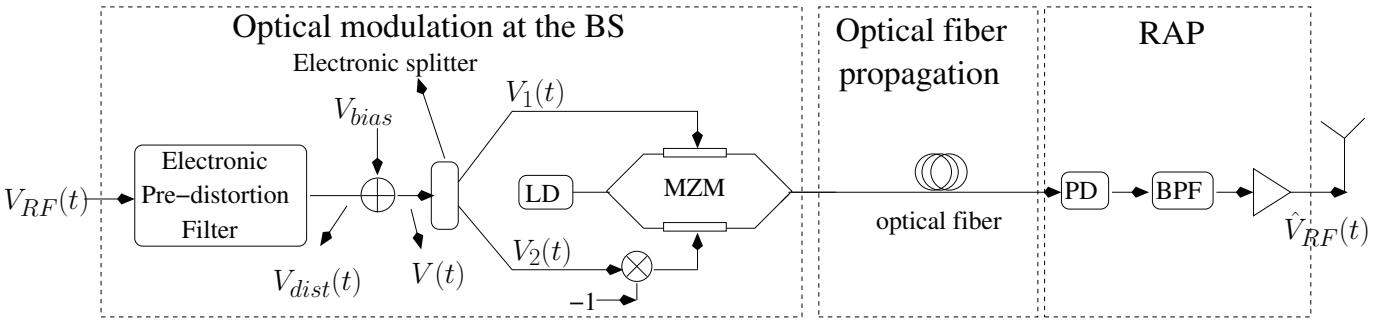

Fig. 3. Block diagram of an RoF link

In (14), the modulated optical signal has an envelope of $A(z,T)$ after propagation through z meters of optical fiber with an attenuation parameter of α, non-linearity parameter of γ and dispersion parameter of D. Additionally, in (14), we have $\beta_2 = D\frac{2\pi c}{\omega_c^2}$, while $T = t - \frac{z}{v_g}$ is the time-axis that moves at a velocity of v_g, c is the speed of light in vacuum and finally, v_g is the envelope's propagation velocity.

Fiber attenuation is a consequence of the Rayleigh scattering of light as well as of material absorption. After propogation through fiber, the optical power $P(z)$ is mathematically expressed as follows [19]:

$$P(z) = P_{laser}\, e^{-\alpha z}. \tag{15}$$

Furthermore, the modulated optical signal has multiple optical frequencies, each of which experiences a different refractive index $n(\omega)$, where an optical signal's propagation velocity is $v_p(\omega) = c/n(\omega)$. Thus, the optical signal's propagation velocity is dependent on its frequency, thereby resulting in fiber-induced dispersion [19].

Furthermore, the fiber-induced non-linearity is a consequence of having a refractive index, which is dependent on the optical power of the propagating signal [19]. Consequently, the time-varying nature of the instantaneous power gives rise to a time-varying refractive index, which induces undesired phase-modulation in the propagating optical signal, which is termed as Self-Phase Modulation (SPM) [19]. We invoke a numerical solution of the NLS expression in Equation (14), namely the Split Step Fourier Transform (SSFT) technique, which relies on sequentially propagating the optical signal through the fiber in small steps [19].

3) Photo-detection: The optical signal exiting the optical fiber is converted to an electronic signal using photo-detection at the RAP. If the optical signal received at the RAP has a field of $E_{received}(t)$, then the photo-detected electronic current $I(t)$ is proportional to the intensity of the received optical signal. In other words, $I(t) = R\,|E_{received}(t)|^2 + n(t)$ [19], where $n(t)$ is the noise imposed by the RoF link, which includes the Relative Intensity Noise (RIN) added by the laser as well as the thermal noise, the dark current noise and the shot noise inflicted by the photo-detector [19].

Since optical intensity modulation was used at the BS in our proposed DL system, the photo-detected signal represents the RF signal transmitted by the BS. After photo-detection, the RF signal $\hat{V}_{RF}(t)$ that is received at the RAP is amplified, filtered using a Band Pass Filter (BPF) and then transmitted to the MS over the wireless channel.

D. Receiver Processing

At each MS k, the signal received at each antenna is sampled at R_s samples/sec and down-converted to baseband. An integrate and dump filter (IDF) is used for recovering the baseband OFDM vector $\boldsymbol{Y}_{ki}[n]$ of components $Y_{ki}[n]$, with $n = 1 \ldots N_{OFDM}$. The signal is down-sampled by a factor of N_{IDF}, where N_{IDF} samples are added together to obtain each of the new samples at a lower sampling frequency equal to R_s/N_{IDF}. The choice of N_{IDF} is important, as will be shown in Section III, since a large value improves the SNR by noise averaging, which requires a higher initial sampling frequency R_s and thus a higher complexity of the receiver. After cyclic prefix removal, the OFDM signals $Y_{ki}[n]$ are demultiplexed for recovering y_{ki}^p, which are the components of the precoded vector $\boldsymbol{y}_k^p$ as follows:

$$y_{ki}^p = \frac{1}{N_{OFDM}} \sum_{n=1}^{N_{OFDM}} Y_{ki}[n] e^{\frac{j2\pi}{N_{OFDM}} np}. \tag{16}$$

The signal received at each MS is processed as shown in Equation (7). However, due to the RoF transmission, Equation (6) will not be satisfied and some residual interference will be present. An adequate design of the RoF link will ensure that this interference is sufficiently low.

III. Design of the RoF link

The main parameters of the RoF link are shown in Table I. The values of $P_{laser} = 15$ dBm and $MDV = 0.5V_\pi$ have been found by simulation to offer the best performance in terms of minimizing the distortion caused by the RoF link.

TABLE I
Design parameters for the RoF link.

Centre Frequency f_0	2 GHz
Optical wavelength λ_c	1,550 nm
Optical frequency f_c	193.5 THz
Transmit Power P_{laser}	0-15 dBm
RIN power spectral density	-154 dBc/Hz
MZM Extinction Ratio ε	30 dB
MZM Insertion Loss t_{attn}	2 dB
MZM Switching Voltage V_π	6 volt
Maximum Drive Voltage MDV	0 V_π volt
Fiber Length L	5 km
Fiber Attenuation Parameter α	0.2 dB/km
Fiber Non-linearity γ	1.2 /W/km
Dispersion Parameter D	16 ps/(km ×nm)
Photo-receiver Amplifier Noise Figure	6 dB

The choice of the parameter N_{IDF} is illustrated in Figure 5, where the mean squared error (MSE) of the received Quaternary Phase Shift keying (QPSK) signal after Orthogonal Frequency Division Demultiplexing (OFDD) of Equation (16) at each MS is shown, when

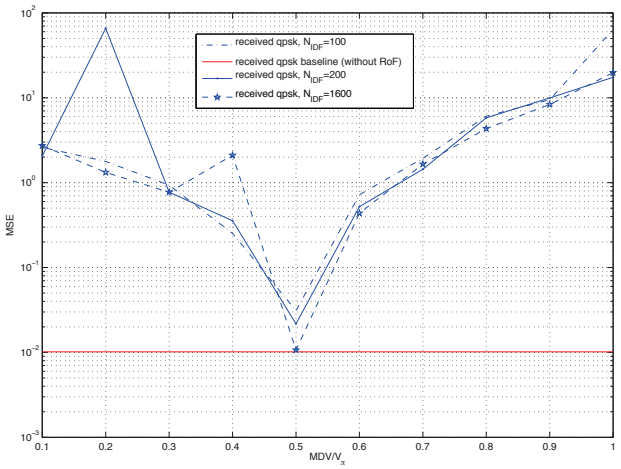

Fig. 5. **Effect of the parameter N_{IDF} on the MSE of the received QPSK signal after OFDD, SNR=20dB.**

the RoF link is used for distributing the precoded signals to the RAPs. This value is shown in comparison to the reference MSE due only to the receiver's AWGN, when the effect of the RoF link is not included. We can see that a value of $N_{IDF} = 200$ represents a good compromise between the performance achieved and the complexity imposed, because the MSE is only increased from 0.01 to 0.02 at its minimum value, which only causes a modest performance degradation, as will be confirmed in the following section. Increasing the value to $N_{IDF} = 1600$ would produce an MSE value extremely close to the reference of 0.01. However, this requires a high sampling frequency at the receiver. Thus, a value $N_{IDF} = 200$ will be used for the performance analysis in the following section. Furthermore, we can see that the lowest MSE is always obtained for $V_{max} = 0.5V_{\pi}$, also confirming the choice of this value.

IV. Performance Evaluation

In this section we analyze the attainable performance in terms of the bit error ratio (BER) of the signal received at each MS in the cluster, where 7 RAPs are jointly transmitting to 7 MS. The modulation of the OFDM subcarriers is QPSK. Each user's data stream is encoded with a 1/3-rate Turbo Code as defined in the LTE standard [16] in conjunction with a variable interleaver length IL. A random external interleaver is added in order to disperse the bursty errors.

In the LTE standard, the subcarriers are grouped into Resource Blocks (RB), where each RB is composed of 12 subcarriers in the frequency domain. The LTE system provides several options for the signal bandwidth, including 1.4, 3, 5, 10, 15 and 20 MHz, while the number of RBs N_{RB} depends on the chosen bandwidth of 6, 15, 25, 50, 75 and 100 RBs, respectively. For the results presented in this section, unless otherwise stated, the total bandwidth used is 5 MHz and consequently we have $N_{RB} = 25$.

In each simulation trial, the positions of the users inside each cell are randomly set according to a uniform distribution. For each pair of transmit-receive antennas, the channel is randomly generated in order to model Rayleigh fading, in conjunction with a path loss that depends on the distance between the transmitter and receiver and has an exponent of 3.8 along with lognormal shadowing of variance 8 dB. The channel is assumed to be the same for the subcarriers of each RB and faded independently between different RBs. No spatial correlation is considered. Additionally, the out-of-cluster interference is modeled as noise under the assumption of the central-limit theorem. Furthermore, the distance between neighbouring cells is set to 1 km, i.e. we have $Rcell = 1/\sqrt{3}$ km and the fiber length from each RAP to the BS is set to 5 km. Finally, the carrier frequency used is set to $f_0 = 2$ GHz.

Figure 6 shows the BER performance for two choices of the value of the interleaver length IL, when the number of TAs and RAs is $t = r = 2$. We can see that, as expected, a longer IL produces a better performance. Additionally, in both cases we can see that the degradation imposed by the RoF link is small compared to a baseline QPSK system using a perfect RoF link.

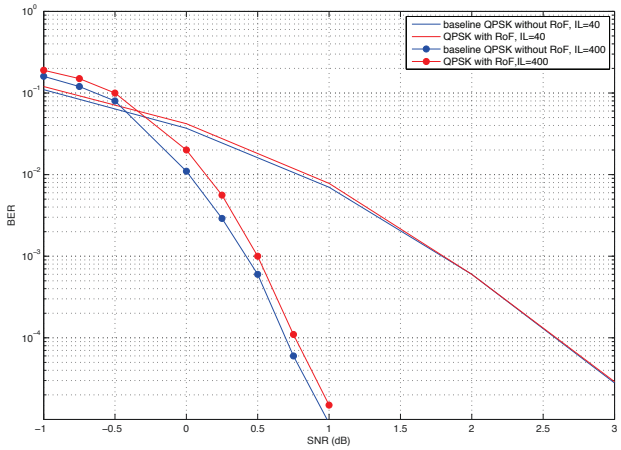

Fig. 6. **Effect of the interleaver length IL on the BER performance, $t = r = 2$.**

The effect of having different number of TAs and RAs is shown in Figure 7. The higher the number of antennas, the more sensitive the system becomes to the interference caused by the non-ideal behavior of the RoF link, and this translates to a higher BER, when compared to the baseline performance relying on a perfect backhaul, as shown in the figure (note that for the SNR definition of Equation (3), the baseline performance is independent of the number of TAs and RAs for $t = r$). However, even for the case of $t = r = 8$, we can see that the SNR degradation is about 1.2 dB, which is quite reasonable. The performance may be further improved by increasing N_{IDF}.

Even though a fiber length of 5 km has been used for obtaining the results provided in this paper, we have verified that the same results and conclusions apply up to a length of 30 km. This is due to the fact that the degradation of the wireless link dominates over the degradation imposed by the RoF link. With the modulation and coding schemes used as well as the parameters of the LTE standard of 5 MHz bandwidth, the average data rate per user for N_{OFDM} subcarriers becomes 16.8 Mbps for $t = r = 2$, 33.6 Mbps for $t = r = 4$ and 67.2 Mbps for $t = r = 8$. Our simulation results show that the small degradation introduced by the RoF link does not significantly change, when the signal bandwidth is increased to 20 MHz, as shown in Figure 8. In the case of $t = r = 8$, these parameters result in a rate of up to 268.8 Mbps.

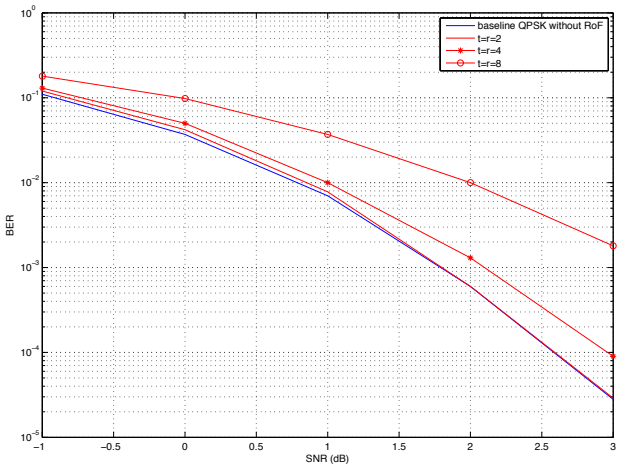

Fig. 7. **BER performance for different number of transmit and receive antennas.**

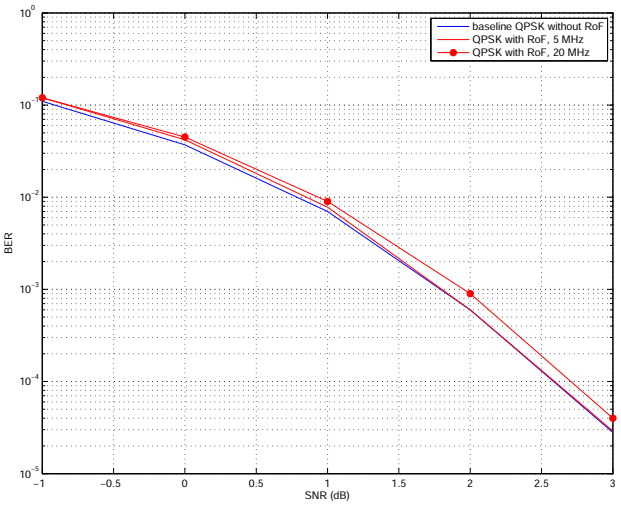

Fig. 8. **BER performance for different bandwidth of the OFDM signals.**

V. Conclusions

We have presented a beneficial RoF design for the cooperation of a set of RAPs. A BS performs transmit precoding using the BD based scheme in conjunction with the knowledge of the channel state information and the users' data and forwards the precoded OFDM DL signal through the RoF link to each transmitting RAP. With the adequate design of the system parameters, including the proposed signal pre-distortion to overcome the non-linearity of the RoF, we have shown that the degradation of the proposed system with respect to an ideal system with perfect backhaul remains modest. Quantitatively, for a Long Term Evolution (LTE) standard MIMO-OFDM signal of bandwidth 5MHz - 20 MHz and for a fiber length up to 30 km, it is possible to transmit at a rate up to 268.2 Mbps to 7 users from 7 coordinated RAPs with a maximum SNR degradation of around 1.2 dB compared to a baseline system relying on a perfect RoF backhaul.

References

[1] G.J. Foschini and M.J. Gans, "On Limits of Wireless Communications in a Fading Environment When Using Multiple Antennas," *Wireless Personal Communications*, Vol. 6, No. 3, pp. 311–335, Mar. 1998.

[2] D. Gesbert, S.G. Kiani, A. Gjendemsjø, and G.E. Øien, "Adaptation, Coordination, and Distributed Resource Allocation in Interference-Limited Wireless Networks," *Proceedings of the IEEE*, Vol. 95, No. 12, pp. 2393–2409, Dec. 2007.

[3] S. Shamai (Shitz) and B.M. Zaidel, "Enhancing the cellular downlink capacity via co-processing at the transmitting end," *Proceedings of IEEE Vehicular Technology Conference*, Rhodes, Greece, pp. 1745–1749, May 2001.

[4] M.K. Karakayali, G.J. Foschini and R.A. Valenzuela, "Network coordination for spectrally efficient communications in cellular systems," *IEEE Wireless Communications*, Vol. 13, No. 4, pp. 56–61, Aug. 2006.

[5] G.J. Foschini, K. Karakayali and R.A. Valenzuela, "Coordinating multiple antenna cellular networks to achieve enormous spectral efficiency," *IEE Proceedings Communications*, Vol. 153, No. 4, pp. 548–555, Aug. 2006.

[6] 3GPP TR 36.814, "Evolved Universal Terrestrial Radio Access (E-UTRA); Further advancements for E-UTRA physical layer aspects," Release 9, v. 9.0.0, Mar. 2010.

[7] Q. H. Spencer, A. L. Swindlehurst and M. Haardt, "Zero-Forcing Methods for Downlink Spatial Multiplexing in Multiuser MIMO Channels," *IEEE Transactions on Signal Processing*, Vol. 52, No. 2, Feb. 2004

[8] J. Zhang, R. Chen, J.G. Andrews, A. Ghosh, and R.W. Heath, "Networked MIMO with Clustered Linear Precoding," *IEEE Transactions on Wireless Communications*, Vol. 8, No. 4, pp. 1910–1921, Apr. 2009.

[9] J. Zhang, R. Chen, J.G. Andrews, A. Ghosh, and R.W. Heath, "Networked MIMO with Clustered Linear Precoding," *IEEE Transactions on Wireless Communications*, Vol. 8, No. 4, pp. 1910–1921, Apr. 2009.

[10] R. Corvaja, J.J. García Fernández and A. García Armada, "Mean Achievable Rates in Clustered Coordinated Base Station Transmission with Block Diagonalization," *IEEE Transactions on Communications*, Vol. 61, No. 8, pp. 3483–3493, Aug. 2013.

[11] "Small cell market status," Informa, December 2012, http://www.smallcellforum.org/.

[12] A. García Armada, M. Sánchez-Fernández and R. Corvaja, "Constrained Power Allocation Schemes for Coordinated Base Station Transmission using Block Diagonalization," *EURASIP Journal on Wireless Comm. and Networking*, DOI: 10.1186/1687-1499-2011-125.

[13] D. Wake, A. Nkansah, and N. J. Gomes, "Radio Over Fiber Link Design for Next Generation Wireless Systems," *Journal of Lightwave Technology*, Vol. 28, No. 16, pp. 2456–2464, Aug. 2010.

[14] G. Gordon, J. Carpenter, M. Crisp, T. Wilkinson, R. Penty and I. Whitel, "Demonstration of radio-over-fibre transmission of broadband MIMO over multimode fibre using mode division multiplexing," *Proceedings of 38th European Conference and Exhibition on Optical Communications*, Amsterdam, Netherlands, pp. 1–3, Sep. 2012.

[15] 3GPP TS 36.104, "Evolved Universal Terrestrial Radio Access (E-UTRA); Base Station (RAP) radio transmission and reception", Release 12, v. 12.1.0, Sep. 2013.

[16] 3GPP TS 36.212, "Evolved Universal Terrestrial Radio Access (E-UTRA);Multiplexing and channel coding," Release 11, v. 11.3.0, Jun. 2013.

[17] J.M. Cioffi, "Advanced Digital Communications, EE379c," Stanford University Course Notes, http://www.stanford.edu/class/ee379c

[18] Y. Chiu, B. Jalali, S. Garner and W. Steier "Broad-band electronic linearizer for externally modulated analog fiber-optic links," *IEEE Photonics Technology Letters*, Vol. 11, No. 1, pp. 48–50, Jan. 1999.

[19] G. P. Agrawal, "Fiber-Optic Communication Systems," *Wiley Publications*, Third Edition, 2002.

[20] C. Lim, A. Nirmalathas, Y. Yang, D. Novak and R. Waterhouse, "Radio-Over-Fiber Systems," *IEEE Communications and Photonics Conference and Exhibition*, pp. 1–10, Nov. 2009.

[21] V. A. Thomas, S. Ghafoor, M. El-Hajjar and L. Hanzo, "A Full-Duplex Diversity-Assisted Hybrid Analogue/Digitized Radio Over Fibre for Optical/Wireless Integration," *IEEE Communications Letters*, pp. 409–412, Feb. 2013.